Sakarya University Journal of Science

ISSN : 2147-835X
Publisher : Sakarya University

Vol. 28, No. 1, 10-19, 2024
DOI: https://doi.org/10.16984/saufenbilder.1345395

Research Article

Drag Reduction on Microstructure Surfaces

Ahmet Ilyas Kodal[1], Şule Kapkın[1*], Hasan Rıza Güven[1]

[1] Istanbul University – Cerrahpaşa, Faculty of Engineering, Department of Mechanical Engineering, Istanbul, Türkiye, ahmetilyas.kodal@ogr.iuc.edu.tr, skapkin@iuc.edu.tr, hrguven@istanbul.edu.tr
[*]Corresponding Author

ARTICLE INFO

Keywords:
Bird Feather
CFD
Drag Reduction
Surfaces
Riblet.

ABSTRACT

In this study, experimental work in the literature about friction on bird-feather like structures has been reviewed and one of these was modeled by using CFD (Computational Fluid Dynamics) to obtain minimum grid parameters. Coupled with obtained optimal grid parameters, the shear stresses of the two-dimensional models were investigated at the values of Reynolds number 110,000-470,000. Based on the concluded previous study, three-dimensional geometries were modeled with reference to two-dimensional models and analyzed with the determined grid structure. The results of the analysis are compared with those of the previous experimental study in the literature. In the final phase of the study, a drag reduction was found to be approximately 30% on the surfaces inspired by bird feathers.

Article History:
Received: 17.08.2023
Accepted: 17.10.2023
Online Available: 27.02.2024

1. Introduction

Reducing the friction at surfaces is an important problem for many industries especially in transportation where fuel consumption and speed are both important parameters. Total drag can be reduced not only by optimizing the form of the body, but also by changing the surface structure so as to reduce viscous friction. In this regard, there have been studies conducted with the inspiration coming from shark skin and bird feathers. Shark skin inspired surfaces reduce drag by up to 10%, while bird feather inspired surfaces are up to 20%.

Reducing drag allows the objects to spend less energy, move faster and cover a longer distance and have higher efficiency. For example, the fuel consumption of land vehicles, air crafts and ships can be reduced by reducing drag. It was reported that covering 70% of the surfaces of Boeing and Airbus planes with the rough surface structures reduced fuel consumption by 1% [1].

Friction at surfaces can be reduced greatly by making micro-scale changes at the surface. Many methods have been developed for accomplishing this; micro-grooved surface structures employed by Pulles (1988), and micro-ballonet structures made by Kodama et al. (2005) can be given as examples. Many similar methods have been developed and each method reduces drag at various levels [2, 3].

It is a known fact that the surfaces of flying organisms evolved in the form of microstructures which would give the most appropriate shape for drag re- duction. For example, microstructures of shark skin influence reducing turbulence and drag on which much work has been done [4].

Cite as: A. I. Kodal, S. Kapkın, H. R. Guven (2024). Drag Reduction on Microstructure Surfaces, *Sakarya University Journal of Science,* 28(1), 10-19. https://doi.org/10.16984/saufenbilder.1345395

Longitudinal prominent and discrete surfaces at unusual sizes and angles which were designed and used at oil-channel experiments by Bechert et al. (1997) achieved maximum 8,7% drag reduction [1]. Walsh and Lindemann (1984) found that 8% drag reduction occurred by copying the microstructure of shark skin to the surfaces (at the value of s+=15) by his work which was also called the effect of shark skin. This s+ is the dimensionless distance among the micro riblets and calculated with the formula $s+ = sV\tau/\nu$.s refers to the distance among the riblets, $V\tau$ refers to the friction velocity and the ν denotes viscosity. Friction velocity is expressed as $V\tau = /(\tau 0/\rho)$, it is related to shear stress on smooth surfaces [5].

To examine the effect of the surface shape on the friction resistance, Bourisli and Al-Sahhaf (2008) analyzed friction coefficient and velocity by a series of simulation tests using riblets in three different directions, square, triangular and semi-circular. As a result, they found that three of the rough surfaces gave less resistance to smooth surfaces and that the triangular riblets provided the greatest drag reduction [6]. Using the simulation software, El-Samni et al. (2007) determined the pressure gradient to compensate for mass flow on smooth sur- faces such as curved surfaces at different protrusions and grooves. This system was used to geometrically optimize gaps between protrusions and protrusions in relation to drag reduction, and a reduction of 11% drag was achieved in these studies [7]. Ren et al. (2005) studied bionic smooth surface evaluation in bending surface design [8]. In different sizes, smooth surfaces carrying a convex body, pits and protrusions were subjected to low speed, subsonic and supersonic wind tunnel tests. The results show that all of the tested smooth surfaces give reduced resistance and the highest drag reduction rate is about 5%. To illuminate the mechanisms underlying drag reduction on smooth surfaces, Sirovich and Karlsson (1997) tested the change in drag reduction on V-shaped grooved surfaces in the wind tunnel. They have found that turbulence energy distribution is reduced by drag reduction and that a reduction in turbulence energy distribution may be a mechanism used by the rough surface approaches [9]. In their study, Bullen and McKenzie (2008) observed that 23 of bat species living in Western Australia could reduce the drag resistance of rough-surfaced areas on the head and body skin of high-speed flying species by 10% [10].

Birds are another class of organisms with micro-structured surfaces. It is known that flight movements and soaring patterns of birds are in the form to minimize the drag force. The microstructure of birds feathers reduces drag significantly. Birds have developed excellent structures by means of evolution along millions of years such as hollow feather shafts and an aerodynamic shape for increasing the flying performance. The alignment of the riblets along the shafts on each wing is a typical feature of bird feathers. This provides the nerds of birds feathers to be attached perfectly especially for major and minor feathers of wings. It is assumed that riblets on such microstructures on feathers reduce drag strongly [11].

Much work has been done on the prepared surfaces which have been inspired by the microstructures of the feathers. In the experimental work made by Tucker and Parrott (1970), Harris falcons floated freely in the air tunnel and they measured the minimum drag with trimming or without trimming the tip feathers of falcons. As a result, they found that trimmed falcons increased drag by 70-90% [12].

Nachtigall (1998) found that, the smooth starling model he used experimentally in the air tunnel has 14% lower drag than the starling model [13]. Figure 1 shows the Starling's position in the wind tunnel. In an experiment in the water tunnel, Chen et al. (2014) observed that the height/width ratio of the drag in three different geometric shapes and dimensions that was inspired by bird feather is the best at 0.6 and reduces the drag up to 21% [14]. Zhou (2006) examined the rough surface of pigeon feather. The placement of the smooth surfaces with protrusions behind the rotary gantry has resulted in a drag reduction of 16.56% as measured by the simulation test [15].

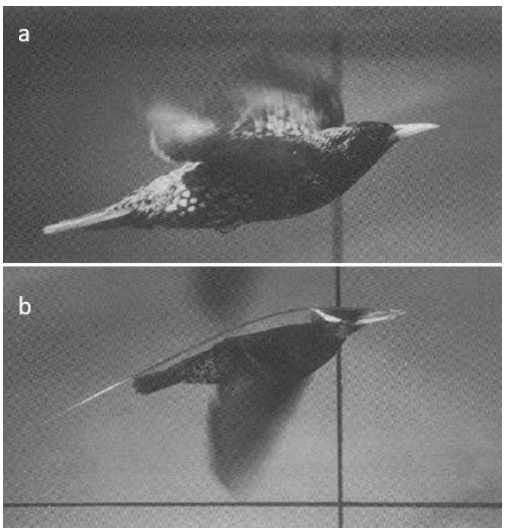

Figure 1. (a) Starling, flying horizontally in wind tunnel, (b) same starling and wind tunnel conditions, the starling wearing a respiration mask [13]

The present study aims to examine micro-grooved structures in varied sizes. The change in drag is examined in three stages on artificial surfaces inspired by the structure of pigeon feather. In the first stage, the experiment by Chen et al. (2013) were modeled in the CFD environment under the same inception and boundary conditions. The purpose of this step is to determine the differences between the experiment and CFD results [16]. In the second step, the effect of geometric dimensions and shapes of riblets on drag is examined by changing height, width and geometric shapes and dimensions, and the optimum parameters are determined. Finally, the change in drag by changing s+ rate is computed for this optimum shape. This study shows that designing new models of various sizes and geometries can further reduce the drag.

1.1. The Structure of bird feathers

Although the structure of bird feathers changes according to the species, the general features are similar. Feather geometry evolved according to the environmental conditions in different geographical regions and reached the most suitable structure. The wings covered with feathers are flighting mechanisms of birds. The wings have changing drag values on different wing surface and wing width ratios [17].

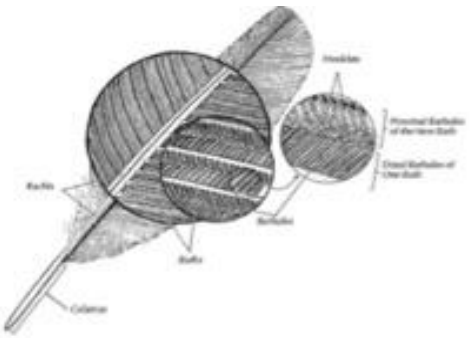

Figure 2. Microscopic appearance of flight feather [18]

Microscopic examination of the feather structure shows that feather nerds are aligned bilaterally along the shaft. The strings between the adjacent nerds run correspondingly along the nerd. As seen in Figure 2 by locating the inner and outer sides up to the shaft, the microstructure strings form the feather riblets. Due to the micro grooved protruding structures on the feather, riblets interact with the flow and crossflow velocity fluctuations occur through riblet holes. These fluctuations affect surface shear stress and momentum transfer positively and reduce drag. Although the distance between the strings, s, is the same everywhere, the height of strings, h, goes down as one moves away from the nerd. Generally, the rate of h/s of the feathers changes between 0.2 and 0.9.

2. Numerical Methods

2.1. Turbulence model

The turbulence model has immense importance in computational studies. The choice of turbulence model changes depending on flow geometry. A study comparing results obtained by using different turbulence models with the experimental results was carried out by Shi et al. (2016). The mentioned study concluded that RNG turbulence model with k-ε equations was the one that gave the closest results to the experimental values [19].

RNG turbulence model with k-ε equations gives better results for rapidly strained flows and swirling flows [19]. RNK k- ε model can be written as

$$\frac{\partial}{\partial t}(\rho k) + \frac{\partial}{\partial x_i}(\rho k u_i) = \frac{\partial}{\partial x_j}\left(\alpha_k \mu_{eff} \frac{\partial k}{\partial x_j}\right) + G_k + G_b - \rho\varepsilon - Y_M + S_k \quad (1)$$

$$\frac{\partial}{\partial t}(\rho\varepsilon) + \frac{\partial}{\partial x_i}(\rho\varepsilon u_i) = \frac{\partial}{\partial x_j}\left(\alpha_\varepsilon \mu_{eff}\frac{\partial \varepsilon}{\partial x_j}\right) + C_{1\varepsilon}\frac{\varepsilon}{k}(G_k + C_{3\varepsilon}G_b) - C_{2\varepsilon}\rho\frac{\varepsilon^2}{k} - R_\varepsilon + S_\varepsilon \quad (2)$$

$C_{1\varepsilon}$, $C_{2\varepsilon}$ and $C_{3\varepsilon}$ are model constants. G_k represents the kinetic energy due to the average velocity. Y_m represents the contribution of the fluctuating dilatation in compressible turbulence to the overall dissipation rate, the quantities αk and $\alpha\varepsilon$ are the inverse effective Prandtl numbers for k and ε, respectively. S_k and $S\varepsilon$ are user-defined source terms.

2.2. Drag calculations

The drag reduction is characterized by the surface friction coefficient differences between the selected reference surface and the tested surface. The drag reduction ratio (DR) is calculated by using the experimental value of Chen et al. (2013) and CFD value by the formula [16]:

$$\%DR = \frac{\Delta\tau}{\tau} = \frac{F_c - F_r}{F_r} \quad (3)$$

Here, Fc is the friction coefficient of structured surface, Fr is the friction coefficient of reference surface (smooth surface). The difference between the shear stress on the reference surface and the shear stress on the tested surface is denoted $\Delta\tau$. The negative value of DR shows that drag decreases, while the positive value shows that drag increases.

3. Numerical Methods

3.1. Comparing the results of experiment and CFD

This section compares the experimental data of Chen et al. (2013) using water tunnel with the CFD results under the same boundary and initial conditions which the structural parameters of bio-inspired herringbone was set as following values [16]: s=100m, h/s=0.6, = 60. And, the length of horizontal empirical surface 0.04 with the generated riblet surface which 0.03 riblet surface along. The water tunnel which was used for the experiment, the total test tube length was 0.6 m and the distance between the two-low pressure measuring holes was 0.5 m, and the test surface was covered in the tube as bonding the skins.

The turbulent tube flow that comes to the test room at constant temperature is completely improved. Figure 3 shows the computational environment of the models used along with representative figure experimental skin which was used in conducted tests. Also, the model test surface is considered flat and other boundary conditions were practically identical. The 1,5% margin of error inflicted of bending the test surface in the experiment is considered in the analysis results and while calculating this difference is also considered.

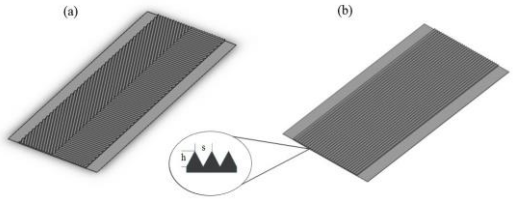

Figure 3. Bird feather model (a) and traditional model, (b) used in Chens experiment

For the different s+ values from the result of the analysis, changing the drag reduction values of the three models was compared with the results of the experiment. There is a 1-2% difference between the experimental results and the analysis results, this difference consists of the mesh number and variations inflicted on bonding the test surface in the experimental setup. Furthermore, the difference could occur due to an adverse effect of surface wrinkling. In this preliminary study, since the grid structure of the model captures the experimental results, this grid structure is also used in the newly developed models.

The results obtained from two different models show that the amount of drag reduction changes depending on the surface skin riblet replacements. It has been evidently concluded that V-shaped skin has greater influence at reducing the drag force as calculated data derived with the same input values other than skin replacement. Consequently, with a higher value of drag reduction, V-shaped riblet skin is employed in subsequent analyses. In the work by

Dean and Bhushan (2010) the effects of variation of the h/s ratio on riblets were examined. Based on the result obtained by Dean and Bhushan (2010), h/s ratio critical impact, as well as skin replacement, led the research to focus in examination to various h/s ratio model with the same riblet adjustment as a support that the total amount of drag reduction can be increased by regenerating ratio [20]. The results of CFD and H. Chens experiment in Figure 4.

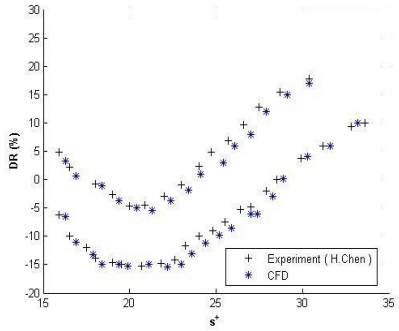

Figure 4. The results of CFD and H. Chens experiment

3.2. The effects of surface feature's size and shapes on Drag - Dimension effects

At this stage, firstly, models are designed as 2 dimensional in varied sizes and shapes. According to the results obtained from 2-dimensional analysis, the value of apical angle being kept constant, the effects of the dimensions and shapes of riblets on drag reduction is evaluated at the second stage. Models that gave reliable results at the end of analysis are redesigned as 3 dimensional models. Designed 3 dimensional models were analyzed in computer environment and the reduction in drag for different s+ values examined.

3.3. Examination on 2 dimensional geometries

On prepared models inspired by the bird feather structure, drag values change by the geometric measures of the feather structure. The change in shear stress due to the geometric shape of the riblet, its height h and width s, was studied. The geometric features that would be used in 3 dimensions were determined by optimizing geometries that were created on two dimensions (Figure 5). The geometric shapes of the models used are shown below. The total length of the models is all 0.0022 m.

The change in shear stress with width and height are examined initially by changing width values s at constant height values h, and then with constant width and changing height of different prepared geometric shapes of models. Dimensions of the models are shown in Table 1.

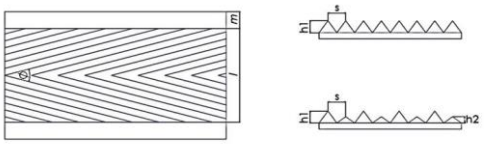

Figure 5. The schematic view of the 3D model

3.4. 3D models

E2 and B2 models which gave appropriate results in two-dimensional analysis were carried onto 3 dimensional models and were analyzed using the Fluent program. The E2 model which was chosen among two-dimensional models was shaped identically and in different dimensions with the riblet of the micro-grooved V-shaped model used in Chen et al. (2013) experiment [16]. The B2 model which gave the best results was formed in different geometric shapes and dimensions. The length and width of the models are taken as 0.035 m. The type of the models are given in Figure 6 and the dimensions are given in Table 2. The riblet of the apical angle in both models is 60 degrees. The riblets were mutually aligned, and the angle denoted as φ is 60 degrees. The height of flow area was taken 20 times more than the height of riblet.

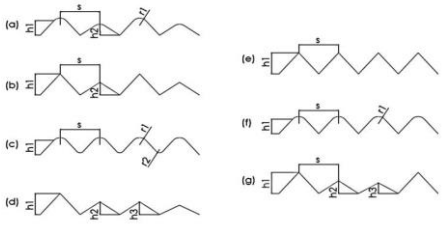

Figure 6. (a) type A model (b) type B model (c) type C model (d) type D model (e) type E model (g) type G model

3.5 Mesh resolution

Models were meshed by observing the y+ value was less than 1 with the analysis mesh and ICEM CFD. All 2-dimensional models are made up of about 100.000 calculation elements while 3 dimensional models are made up of 5 million. The height of the calculation area was taken 20 times more than the height of riblet of the model. The general mesh view of the models is shown in Figure 7 and the shear stresses of two-dimensional models are shown in Figure 8.

3.5.1 Mesh structure in two-dimensional model

The Ansys-Mesh program was used for meshing the two-dimensional models. The mesh was created in two stages, first the large cells forming the control volume and then the small cells near the surface. The inlet, outlet and outer surfaces of the flow volume were formed by triangular cells. The middle volume of the flow volume was formed with rectangular cells. The numerical mesh structure was prepared with smaller and denser cells on the surface to be analyzed and larger and sparser cells towards the walls of the flow volume. The reason for creating cells with different sizes and shapes in the flow volume is to ensure faster convergence of the analysis.

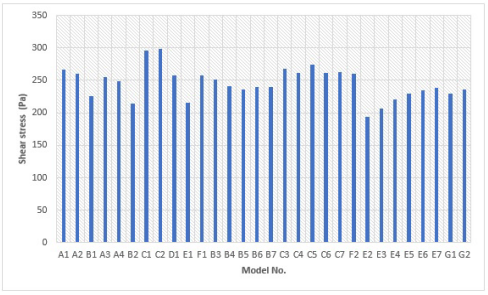

Figure 8. Shear stresses of two-dimensional models

The mesh structure has an average mesh quality of 0.72, with a maximum quality of 1 and a minimum quality of 0.0260. Cells with low mesh quality will have no effect on the analysis since they are not on or near the walls of the flow volume, i.e. on or near the surface to be analyzed.

3.5.2. Mesh structure of the three-dimensional mode

The dimensions of the flow volume were chosen small enough not to disturb the flow in order to reduce the computation time. At the same time,

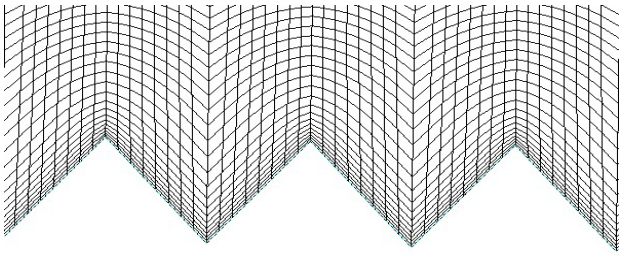

Figure 7. Mesh view of two-dimensional model

the side walls of the flow volume were taken as symmetry to reduce the computation time. Thus, the number of meshes was halved. Most of the cells in the numerical mesh structure were placed in the boundary layer of the surface to be analyzed.

Mesh structures have an average mesh quality of 0.6-0.7, with a maximum quality of 1 and a minimum quality of 0.00267. Cells with low mesh quality will have no effect on the analysis since they are not on the walls of the flow volume, i.e. on or near the surface to be analyzed (Figure 8).

3.6. Analysis of models

Models were analyzed in the ansys-fluent program as time-independent. RNG k-was chosen as the turbulence model with enhanced wall treatment. Water has taken as fluid with the velocity of 1-5 m/s and analyzed separately for each case. The turbulence density taken 5% and the turbulence viscosity ratio taken 5.

Table 1 2D Dimensions of the models

Constant s									
Model No.	h1(μm)	h2(μm)	h3(μm)	s(μm)					
A1	50	20	—	100					
A2	50	26	—	100	10	—	B4	80	60	30
A3	55	25	—	100	5	—	B5	90	60	30
A4	55	31	—	100	5	—	B6	110	60	30
B1	60	30	—	100	—	—	B7	120	60	30
B2	60	36	—	100	—	—	C3	70	50	—
C1	50	—	—	100	10	5	C4	80	50	—
C2	55	—	—	100	5	10	C5	90	50	—
D1	60	58	—	100	—	—	C6	110	50	—
E1	60	—	—	100	—	—	C7	120	50	—
E2	70	—	—	100	—	—	E3	70	60	—
F1	50	—	—	100	10	—	E4	80	60	—
F2	70	—	—	100	—	—	E5	90	60	—
G1	60	30	30	100	—	—	E6	110	60	—
G2	60	36	30	100	—	—	E7	120	60	—

Table 2. 3D models dimension table

Models	L(m)	s(μm)	h1(μm)	h2(μm)
E2-3D	0.03	100	70	—
B2-3D	0.03	100	60	36

Fluid particles do not slip because the velocity of the fluid contacting parts of the wall is zero. For this reason, a no-slip condition is preferred for the flow volume walls and the surface to be analyzed. In 3D models, the sides are symmetrical and the outlet pressure is equalized to the atmospheric pressure (Figure 9). The SIMPLE algorithm was chosen as the solution method and the convergence criterion was taken as 10-5 ($C1_\epsilon = 0{,}43;\ C2_\epsilon = 1{,}92; C3_\epsilon = 0{,}09$). The shear stresses of the models were investigated at the values of Reynolds number 110,000-470,000. Simulate the 3D geometry is shown in Figure 10.

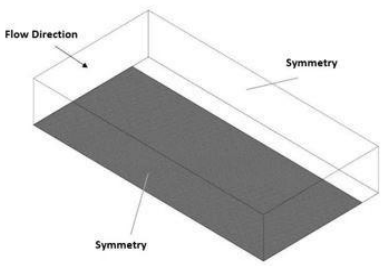

Figure 9. Simulation model of 3D geometries

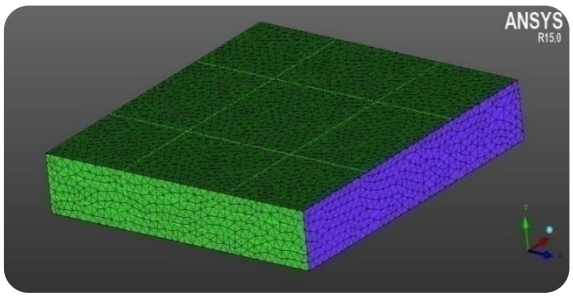

Figure 10. General cross-sectional image of 3D models

4. Results

The validity of the CFD study has been demonstrated by comparison with the experimental work in the literature. Shear stresses, one of the drag reduction parameters, were investigated in 2D models of 30 different sizes and shapes. The comparison of surface shear stresses in models from the analysis is given in Figure 9. It is found that the shear stresses of E2 and B2 models are lower than other models. The velocity vectors of E2 and B2 models near the wall are shown in Figure 11. As seen in the figures swirls interact with the points of riblet and create low-velocity areas in the spaces of holes. These low-velocity areas create low shear stress with the cross-flow velocity fluctuations [3].

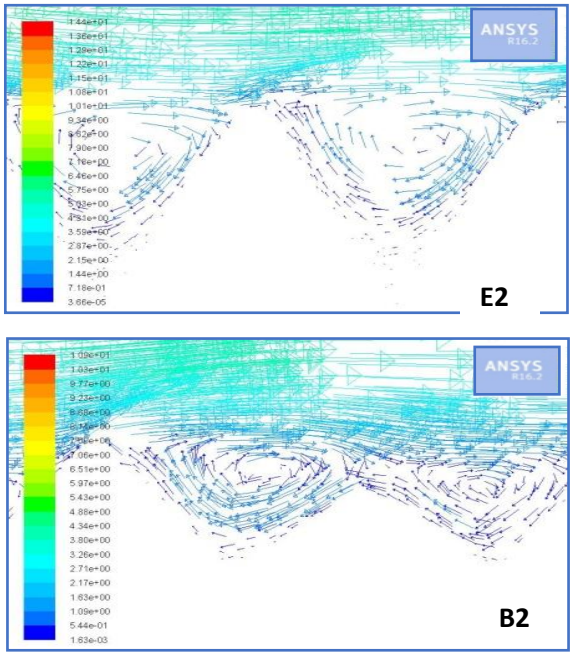

Figure 11. Velocity of E2 and B2 models at the sections near the wall

If these stress values are much at the points of riblet, they stay only in a very small area. Most of the surface area has low surface stress. In this study, in the analysis which has different parameters on geometries shear stresses, initially with the values of geometries which has constant width s, changing height h and constant height h, changing width s are examined. According to the results, it was pointed geometry gave the best results. It has been observed that, the analysis made on this geometry with the constant width and changing height by decreasing the value h provides better results on reducing drag of geometry. It has been observed that, as the height value increases, it affects negatively, and the best result has been taken on 60-70 micrometers.

For the width values as the width increases better results increases parallelly while s value was found to give worse results than values were greater than 120 micrometers. On the prepared B2-3d and E2- 3d models which inspired of 2 dimensional models, alternately from 18% to 30% drag reduction has been found. In Figure 12, the results of Bechert et al. (1997) experimental work with the results of this study about how different s+ values change the drag was compared [1]. The drag reduction for both models was observed to be maximum at $s+ \approx 15$ value.

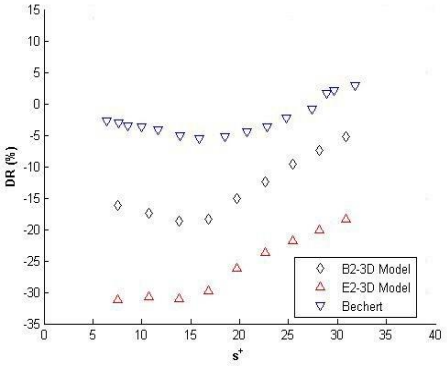

Figure 12. DR/s+ comparison of CFD and Bechert's experiment

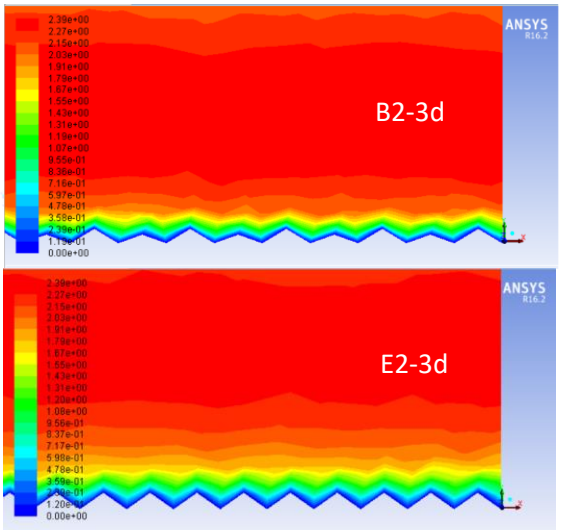

Figure 13. Cross-section velocity contour graphics of the B2-3d and E2-3d models near the wall

As it observed in the cross-section velocity contour, the viscous substratum of the E2-3d model is thicker than the B2-3d model. Consideration of the viscous lower layer removes turbulent swirls from the surface and it works as a drawing compound for the surface drag reduction. B2-3d and E2-3d near wall section velocity contour plots are shown in Figure 13.

5. Conclusion

The CFD studies which were made by using k-ε turbulence model are close to the experimental results. 2-dimensional studies show that riblets that have pointed geometry give better results than the rounded models. In 3-dimensional models drag was reduced by up to 30%. This

study shows that optimizing surface shapes and dimensions achieves good drag reduction.

Article Information Form

Funding
The authors have no received any financial support for the research, authorship or publication of this study.

Authors' Contribution
The authors contributed equally to the study.

The Declaration of Conflict of Interest/ Common Interest
No conflict of interest or common interest has been declared by the authors.

The Declaration of Ethics Committee Approval
This study does not require ethics committee permission or any special permission.

The Declaration of Research and Publication Ethics
The authors of the paper declare that they comply with the scientific, ethical and quotation rules of SAUJS in all processes of the paper and that they do not make any falsification on the data collected. In addition, they declare that Sakarya University Journal of Science and its editorial board have no responsibility for any ethical violations that may be encountered, and that this study has not been evaluated in any academic publication environment other than Sakarya University Journal of Science.

References

[1] D. W. Bechert, M. Bruse, W. Hage, J. G. T. V. D. Hoeven, G. Hoppe, "Experiments on drag-reducing surfaces and their optimization with an adjustable geometry," Journal of Fluid Mechanics, vol. 338, pp. 59–87, 1997.

[2] C. Pulles, "Drag reduction of turbulent boundary layers by means of grooved surfaces," [Ph.D. Thesis 1 (Research TU/e / Graduation TU/e), Applied Physics and Science Education]. Technische Universiteit, 1988.

[3] Y. Kodama, T. Takahashi, M. Makino, T. Hori, T. Ueda, N. Kawamura, M. Shibata, H. Kato, T. Inoue, T. Suzuki, Y. Toda, K. Yamashita, "Practical application of microbubbles to ships --- Large scale model experiments and a new full scale experiment," Int. Sympos. Smart Contr. Turbul., Jan. 2005.

[4] M. Sasamori, H. Mamori, K. Iwamoto, A. Murata, "Experimental study on drag-reduction effect due to sinusoidal riblets in turbulent channel flow," Experiments in Fluids, vol. 55, no. 10, p. 1828, 2014.

[5] M. Walsh, A. Lindemann, "Optimization and application of riblets for turbulent drag reduction," in 22nd Aerospace Sciences Meeting, in Aerospace Sciences Meetings, American Institute of Aeronautics and Astronautics, 1984.

[6] R. I. Bourisli, A. A. Al-Sahhaf, "CFD modeling of turbulent boundary layer flow in passive drag-reducing applications," presented at the Advances In Fluıd Mechanics 2008, The New Forest, UK, May 2008, pp. 79–90.

[7] O. A. El-Samni, H. H. Chun, H. S. Yoon, "Drag reduction of turbulent flow over thin rectangular riblets," International Journal of Engineering Science, vol. 45, no. 2, pp. 436–454, 2007.

[8] L. Q. Ren, C. C. Zhang, L. M. Tian, "Experimental study on drag reduction for bodies of revolution using bionic non-smoothness," Journal of Jilin University (Engineering and Technology Edition), vol. 35, no. 4, pp. 431–436, 2005.

[9] L. Sirovich, S. Karlsson, "Turbulent drag reduction by passive mechanisms," Nature, vol. 388, no. 6644, Art. no. 6644, 1997.

[10] R. D. Bullen, N. L. McKenzie, “The pelage of bats (Chiroptera) and the presence of aerodynamic riblets: the effect on aerodynamic cleanliness,” Zoology (Jena), vol. 111, no. 4, pp. 279–286, 2008.

[11] S. G. Martin, “Fluid Flow Modeling of Biomimetic Structures,” Ph.D. Thesis, Department of Mechanical and Aerospace Engineering at The Ohio State University”, 2013.

[12] V. A. Tucker, G. C. Parrott, “Aerodynamics of gliding flight in a falcon and other birds,” Journal of Experimental Biology, vol. 52, no. 2, pp. 345–367, 1970.

[13] W. Nachtigall, “Starlings and starling models in wind tunnels,” Journal of Avian Biology, vol. 29, no. 4, pp. 478–484, 1998.

[14] H. Chen, F. Rao, X. Shang, D. Zhang, I. Hagiwara, “Flow over bio-inspired 3D herringbone wall riblets,” Experiments in Fluids, vol. 55, no. 3, p. 1698, 2014.

[15] C. Zhou, L. Tian, L. Ren, W. Zhao, R. Zhang, S. Zhang, “Research on non-smooth surface morphology and bionic technology of columba livia feather,” Transactıons of the Chınese Society For Agricultural Machinery, vol. 37, no. 11, pp. 180–183, 2006.

[16] H. Chen, F. Rao, X. Shang, D. Zhang, I. Hagiwara, “Biomimetic drag reduction study on herringbone riblets of bird feather,” Journal of Bionic Engineering, vol. 10, no. 3, pp. 341–349, 2013.

[17] C. J. Pennycuick, “A wind-tunnel study of gliding flight in the Pigeon Columba Livia,” Journal of Experimental Biology, vol. 49, no. 3, pp. 509–526, 1968.

[18] I. J. Lovette W. Fitzpatrick, “Handbook of bird biology, 3rd Ed. | Bird Academy • The Cornell Lab.” 2016.

[19] Z. Shi, J. Chen, Q. Chen, “On the turbulence models and turbulent Schmidt number in simulating stratified flows,” Journal of Building Performance Simulation, vol. 9, no. 2, pp. 134–148, 2016.

[20] B. Dean, B. Bhushan, “Shark-skin surfaces for fluid-drag reduction in turbulent flow: a review,” Philosophical Transactions of the Royal Society A: Mathematical, Physical and Engineering Sciences, vol. 368, no. 1929, pp. 4775–4806, 2010.